Inorganic Chemistry
Article

Inorg. Chem. **2009,** *48,* 4873–4881 **4873**
DOI:10.1021/ic900240y

Copper Coordination Polymers Based on Single-Chain or Sheet Structures Involving Dinuclear and Tetranuclear Copper(II) Units: Synthesis, Structures, and Magnetostructural Correlations

Santokh Singh Tandon,[†] Scott D. Bunge,[‡] Douglas Motry,[†] José Sánchez Costa,[*,§,⊥] Guillem Aromí,[⊥] Jan Reedijk,[*,§] and Laurence K. Thompson[¶]

[†]*Department of Chemistry, Kent State University at Salem, Salem, Ohio 44460,* [‡]*Department of Chemistry, Kent State University, Kent, Ohio 44242,* [§]*Gorlaeus Laboratories, Leiden Institute of Chemistry, Leiden University, P.O. Box 9502, 2300 RA Leiden, The Netherlands,* [⊥]*Grup d'Interaccions Magnètiques, Departament de Química Inorgànica, Universitat de Barcelona, Diagonal 647, 08028 Barcelona, Spain, and* [¶]*Department of Chemistry, Memorial University, St. John's, Newfoundland A1B 3X7, Canada*

Received February 5, 2009

Reactions between the potentially pentadentate (N_2O_3), trianionic double Schiff-base ligand 2,6-bis[[(2-hydroxyethyl)imino]methyl]-4-methylphenol (H_3L) and $Cu(CH_3CO_2)_2$ or $Cu(ClO_4)_2$, in the presence of NaN_3, give novel coordination polymers with chain $\{[Cu_2(H_2L)(N_3)_3]_2 \cdot H_2O\}_n$ (**1**) or sheet $[Cu_2(H_2L)(N_3)_3]_n$ (**2**) and $[Cu_2(HL)(N_3)]_n[ClO_4]_n$ (**3**) structures, respectively. These clusters are comprised of repeating dinuclear units (**1**) or their dimers (**2** and **3**). In these compounds, H_3L acts as a tridentate (N_2O) monoanionic (**1**), tetradentate (ON_2O) monoanionic (**2**), or pentadentate (O_3N_2) dianionic (**3**) ligand. Compound $[Cu_2(HL)(N_3)_2(H_2O)] \cdot 0.5CH_3OH$ (**4**) formed from the reaction of $Cu(CH_3CO_2)_2$ with H_3L under reflux, which did not afford crystals suitable for X-ray studies. X-ray structure determinations have revealed that the basic building block in **1**−**3** comprises two copper centers bridged through one μ-phenolate O atom from H_2L^- or HL^{2-} and one μ-azido(N1,N1) ion. Compounds **1**−**3** unveil three different ways in which this Cu_2 basic unit may be organized in the crystalline phase at the supramolecular level through a variety of bridging interactions involving additional azide ligands or alkoxide groups from the side arms of the ligand H_3L. Bulk magnetization measurements have served to demonstrate that the magnetic interactions are completely dominated by the strong antiferromagnetic coupling occurring within the Cu_2 building block, with coupling constants ranging from 330 to 560 cm^{-1} (in the $H = -JS_1S_2$ convention). These results together have been incorporated with data from the few related copper dimers reported exhibiting the same bridging pattern into a study aimed at extracting possible magnetostructural correlations within this Cu_2 unit. An earlier predicted correlation between J and the angle formed by the phenoxide bridge and the Cu_2 core has been identified for the first time.

Introduction

During the last 2 decades, there has been a growing interest in the synthesis, structural characterization, and magnetic properties of polynuclear spin-coupled clusters of paramagnetic transition-metal ions exhibiting ferromagnetic and antiferromagnetic spin-exchange interactions.[1−5] This surge of interest in polynuclear complexes is because of their potential to provide access to new magnetic materials, which could have a possible use in quantum computing or magnetic refrigeration.[6−8] Indeed, molecular-based magnetic materials have been the subject of many studies in recent years because of their physical properties in low-dimensional magnetic systems; this deals

*To whom correspondence should be addressed. E-mail: j.sanchezcosta@qi.ub.es (J.S.C.), reedijk@chem.leidenuniv.nl (J.R.).

(1) Kahn, O. Molecular Magnetism. In *Molecular Magnetism*, VCH: New York, 1993; p 131.
(2) Miller, J. S.; Epstein, A. J. *Angew. Chem., Int. Ed. Engl.* **1994**, *33*, 385–415.
(3) Ribas, J.; Escuer, A.; Monfort, M.; Vicente, R.; Cortes, R.; Lezama, L.; Rojo, T. *Coord. Chem. Rev.* **1999**, *195*, 1027–1068.
(4) Thompson, L. K. *Coord. Chem. Rev.* **2002**, *233*, 193–206.
(5) Turnbull, M. M.; Sugimoto, T.; Thompson, L. K. *Molecule-Based Magnetic Materials—Theory, Techniques, and Applications*; American Chemical Society: Washington, DC, 1996; Vol. 644.
(6) Christou, G.; Gatteschi, D.; Hendrickson, D. N.; Sessoli, R. *MRS Bull.* **2000**, *25*, 66–71.
(7) Miller, J. S.; Drillon, M. *Magnetism: Molecules to Materials*; Wiley: Weinheim, Germany, 2001.
(8) Wernsdorfer, W.; Sessoli, R. *Science* **1999**, *284*, 133–135.

© 2009 American Chemical Society
Published on Web 4/20/2009

with materials such as single-molecule magnets (SMMs);[9−23] and single-chain magnets.[24−29] A large number of spin-coupled clusters that act as "SMMs" displaying slow magnetization relaxation at low temperature have been prepared, and their magnetostructural correlations were studied.[6−23] This unique behavior of some spin-coupled clusters has been attributed to the molecular properties of a large ground spin state and a large easy-axis-type magnetic anisotropy (negative axial zero-field-splitting parameter, D). Many of the molecular-based magnetic materials display long-range magnetic ordering at room temperature. Some of these materials are based on single metal centers bridged by polydentate ligands as well as doubly or triply bridging anions like N_3^-, NCS^-, CN^-, $C_2H_3O_2^-$, $C_6H_5O^-$, OH^-, etc., to form extended networks.[30−35]

The number of materials involving discrete polynuclear metal complexes as building blocks is limited.[36,37] Manganese is the most abundant transition metal present in the spin-coupled clusters (Mn_4 to Mn_{84}) exhibiting SMM behavior.[38,39] The number of SMM clusters containing metals other than manganese is very limited, and these include iron (Fe_4 to Fe_{19}), nickel (Ni_4 to Ni_{21}), vanadium (V_4), and cobalt (Co_4) clusters.[38,39]

In these spin-coupled clusters, the bridging ligands between paramagnetic centers play a dominant role in determining the nature and strength of the spin-exchange interactions. Out of all of these, azido bridges play an important role as mediators for magnetic exchange interactions between metal centers. Because of flexidentate nature, azido bridges can mediate different types of magnetic interactions between paramagnetic metal ions depending on the mode of their coordination.[3,40,41] In most of the reported clusters, azide bridges propagate antiferromagnetic interactions when they act as end-to-end (EE; μ-1,3) bridges and ferromagnetic behavior when they act as end-on (EO; μ-1,1) bridges.[3,42−44] The number of coordination complexes in which azide ions exhibit novel triply bridging (μ_3-1,1,1 and μ_3-1,1,3) and quadruply bridging (μ_4-1,1,1,1 and μ_4-1,1,3,3) modes is relatively limited.[3,42,43,45−49]

The coordination versatility of Schiff-base ligands (Figure 1) toward transition-metal ions has prompted us to explore the coordination chemistry of a coordinatively more dynamic, conformationally flexible, versatile ligand (H_3L). In this report, the synthesis, crystal structures, and magnetic properties of three new copper coordination polymers with very unusual and interesting single-chain or sheet structures are presented. All complexes exhibit the same type of Cu_2 building block cemented by the phenoxide O atom of the Schiff base and, by monodentate azide, organized in supramolecular architectures through a variety of alkoxide, phenoxide, and azide bridges. The magnetic exchange interactions within complexes **1**−**3** are dominated by the strong antiferromagnetic coupling within the copper dinuclear units. The strength of the coupling in the three compounds has been determined, and the results were used together with literature data from other reported examples in an attempt to establish specific magnetostructural correlations. During the course of this work, the structure of compound **3** appeared,

(9) Brechin, E. K.; Boskovic, C.; Wernsdorfer, W.; Yoo, J.; Yamaguchi, A.; Sanudo, E. C.; Concolino, T. R.; Rheingold, A. L.; Ishimoto, H.; Hendrickson, D. N.; Christou, G. *J. Am. Chem. Soc.* **2002**, *124*, 9710–9711.
(10) Friedman, J. R.; Sarachik, M. P.; Tejada, J.; Maciejewski, J.; Ziolo, R. *J. Appl. Phys.* **1996**, *79*, 6031–6033.
(11) Friedman, J. R.; Sarachik, M. P.; Tejada, J.; Ziolo, R. *Phys. Rev. Lett.* **1996**, *76*, 3830–3833.
(12) Gatteschi, D.; Sessoli, R. *Angew. Chem., Int. Ed.* **2003**, *42*, 268–297.
(13) Sessoli, R.; Gatteschi, D.; Caneschi, A.; Novak, M. A. *Nature (London)* **1993**, *365*, 141–143.
(14) Sessoli, R.; Tsai, H. L.; Schake, A. R.; Wang, S. Y.; Vincent, J. B.; Folting, K.; Gatteschi, D.; Christou, G.; Hendrickson, D. N. *J. Am. Chem. Soc.* **1993**, *115*, 1804–1816.
(15) Thomas, L.; Lionti, F.; Ballou, R.; Gatteschi, D.; Sessoli, R.; Barbara, B. *Nature (London)* **1996**, *383*, 145–147.
(16) Bagai, R.; Wernsdorfer, W.; M., L.-G.; Christou, G. *J. Am. Chem. Soc.* **2007**, *129*, 12918–12920.
(17) Gatteschi, D.; Sessoli, R. *J. Magn. Magn. Mater.* **2004**, *272*−*76*, 1030–1036.
(18) Milios, C. J.; Vinslava, A.; Wernsdorfer, W.; Moggach, S.; Parsons, S.; Perlepes, S. P.; Christou, G.; Brechin, E. K. *J. Am. Chem. Soc.* **2007**, *129*, 2754–2755.
(19) Milios, C. J.; Vinslava, A.; Wood, P. A.; Parsons, S.; Wernsdorfer, W.; Christou, G.; Perlepes, S. P.; Brechin, E. K. *J. Am. Chem. Soc.* **2007**, *129*, 8–9.
(20) Murugesu, M.; Habrych, M.; Wernsdorfer, W.; Abboud, K. A.; Christou, G. *J. Am. Chem. Soc.* **2004**, *126*, 4766–4767.
(21) Soler, M.; Wernsdorfer, W.; Folting, K.; Pink, M.; Christou, G. *J. Am. Chem. Soc.* **2004**, *126*, 2156–2165.
(22) Stamatatos, T. C.; Abboud, K. A.; Wernsdorfer, W.; Christou, G. *Angew. Chem., Int. Ed.* **2007**, *46*, 884–888.
(23) Yang, E. C.; Hendrickson, D. N.; Wernsdorfer, W.; Nakano, M.; Zakharov, L. N.; Sommer, R. D.; Rheingold, A. L.; Ledezma-Gairaud, M.; Christou, G. *J. Appl. Phys.* **2002**, *91*, 7382–7384.
(24) Aliaga-Alcalde, N.; Edwards, R. S.; Hill, S. O.; Wernsdorfer, W.; Folting, K.; Christou, G. *J. Am. Chem. Soc.* **2004**, *126*, 12503–12516.
(25) Caneschi, A.; Gatteschi, D.; Lalioti, N.; Sangregorio, C.; Sessoli, R.; Ventiru, G.; Vendigni, A.; Retoori, A.; Pini, M. G.; Novak, M. A. *Angew. Chem., Int. Ed.* **2001**, *40*, 1760–1763.
(26) Clerac, R.; Miyasaka, H.; Yamashita, M.; Coulon, C. *J. Am. Chem. Soc.* **2002**, *124*, 12837–12844.
(27) Coulon, C.; Clerac, R.; Lecren, L.; Wernsdorfer, W.; Miyasaka, H. *Phys. Rev. B* **2004**, 69.
(28) Coulon, C.; Miyasaki, H.; Clerac, R. *Struct. Bonding (Berlin)* **2006**, *122*, 163–206.
(29) Milios, C. J.; Inglis, R.; Vinslava, A.; Bagai, R.; Wernsdorfer, W.; Parsons, S.; Perlepes, S. P.; Christou, G.; Brechin, E. K. *J. Am. Chem. Soc.* **2007**, *129*, 12505–12511.
(30) Chakov, N. E.; Wernsdorfer, W.; Abboud, K. A.; Christou, G. *Inorg. Chem.* **2004**, *43*, 5919–5930.
(31) Escuer, A.; Aromi, G. *Eur. J. Inorg. Chem.* **2006**, 4721–4736.
(32) Ferbinteanu, M.; Miyasaka, H.; Wernsdorfer, W.; Nakata, K.; Sugiura, K.; Yamashita, M.; Coulon, C.; Clerac, R. *J. Am. Chem. Soc.* **2005**, *127*, 3090–3099.
(33) Massoud, S. S.; Mautner, F. A.; Vicente, R.; Gallo, A. A.; Ducasse, E. *Eur. J. Inorg. Chem.* **2007**, 1091–1102.
(34) Ribas, J. R. I. *Contrib. Sci.* **1999**, *1*, 39–51.
(35) Tasiopoulos, A. J.; Vinslava, A.; Wernsdorfer, W.; Abboud, K. A.; Christou, G. *Angew. Chem., Int. Ed.* **2004**, *43*, 2117–2121.
(36) Eddaoudi, M.; Moler, D. B.; Li, H. L.; Chen, B. L.; Reineke, T. M.; O'Keeffe, M.; Yaghi, O. M. *Acc. Chem. Res.* **2001**, *34*, 319–330.
(37) Roubeau, O.; Clerac, R. *Eur. J. Inorg. Chem.* **2008**, 4325–4342.
(38) Aromí, G.; Brechin, E. K. *Struct. Bonding (Berlin)* **2006**, *122*, 1–67.
(39) Price, D. J.; Batten, S. R.; Moubaraki, B.; Murray, K. S. *Polyhedron* **2007**, *26*, 305–317.
(40) Charlot, M. F.; Kahn, O.; Chaillet, M.; Larrieu, C. *J. Am. Chem. Soc.* **1986**, *108*, 2574–2581.
(41) Thompson, L. K.; Tandon, S. S. *Comments Inorg. Chem.* **1996**, *18*, 125–144.
(42) Demeshko, S.; Leibeling, G.; Maringgele, W.; Meyer, F.; Mennerich, C.; Klauss, H. H.; Pritzkow, H. *Inorg. Chem.* **2005**, *44*, 519–528.
(43) Meyer, F.; Demeshko, S.; Leibeling, G.; Kersting, B.; Kaifer, E.; Pritzkow, H. *Chem.—Eur. J.* **2005**, *11*, 1518–1526.
(44) Meyer, F.; Kozlowski, H. In *Comprehensive Coordination Chemistry*; McCleverty, J. A., Meyer, T. J., Eds.; Pergamon: New York, 2004; pp 247−276.
(45) Boudalis, A. K.; Donnadieu, B.; Nastopoulos, V.; Clemente-Juan, J. M.; Mari, A.; Sanakis, Y.; Tuchagues, J. P.; Perlepes, S. P. *Angew. Chem., Int. Ed.* **2004**, *43*, 2266–2270.
(46) Halcrow, M. A.; Huffman, J. C.; Christou, G. *Angew. Chem., Int. Ed. Engl.* **1995**, *34*, 889–891.
(47) Halcrow, M. A.; Sun, J. S.; Huffman, J. C.; Christou, G. *Inorg. Chem.* **1995**, *34*, 4167–4177.
(48) Ma, D. Q.; Hikichi, S.; Akita, M.; Moro-oka, Y. *J. Chem. Soc., Dalton Trans.* **2000**, *7*, 1123–1134.
(49) Nanda, P. K.; Aromi, G.; Ray, D. *Chem. Commun.* **2006**, 3181–3183.

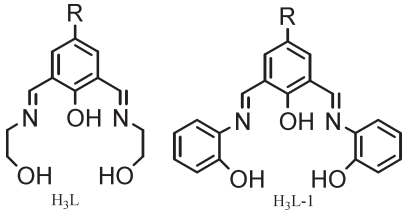

Figure 1. Structures of the Schiff-base ligands.

albeit determined at higher T and with a slightly higher R value.[50] Our data on this compound are listed in the Supporting Information only.

Experimental Section

Physical Measurements. IR spectra were recorded as Nujol mulls using a Perkin-Elmer FT-IR instrument, and UV−vis spectra of the powdered compounds were obtained as Nujol mulls or in solution using a Cary 5E spectrometer. Microanalyses were carried out using a Leco CHNS analyzer. The technique used for copper analysis is as follows: The amount of copper was analyzed using ethylenediaminetetraacetic acid (EDTA) titration. In this method, the complex was decomposed by heating with concentrated nitric acid (3 × 10 mL) to near dryness. The residue was dissolved in water, and an excess of a standard H_2Na_2EDTA solution was added. An excess of EDTA was back-titrated using a standard solution of lead(II) nitrate and xylenol orange as an indicator. Variable-temperature magnetic data (2−300 K) were obtained using a Quantum Design MPMS5S SQUID magnetometer with a field strength of 0.1 T. Background corrections for the sample-holder assembly and diamagnetic components of the complexes were applied.

Materials. 2,6-Diformylphenol was isolated by the reported method,[51] and 2-aminoethanol was supplied by Aldrich. All other chemicals used (solvents and metal salts) were analytical or reagent-grade and were employed without further purification.

Synthesis of the Coordination Compounds. ***Caution!*** *Azide and perchlorate complexes of metal ions involving organic ligands are potentially explosive. Only small quantities of the complexes should be prepared, and these should be handled with care.*

The synthesis of complex **1** was carried out in the presence of excess acetate by adding CH_3COONa, whereas the synthesis of complex **2** was carried out without adding CH_3COONa.

In some cases, there is a small difference between the most reasonable formula based on the elemental analysis (analytical formula) and that obtained from X-ray crystallography. For consistency, the analytical formulas with some MeOH solvent will be used below. For compound **1** the X-ray formula is $\{[Cu_2(H_2L)(N_3)_3]\cdot H_2O\}_n$ and the analysis formula is $\{[Cu_2(H_2L)(N_3)_3]\cdot H_2O\cdot 0.7CH_3OH\}_n$, for compound **2** the X-ray formula is $[Cu_2(H_2L)(N_3)_3]_n$ and the analysis formula is $\{[Cu_2(H_2L)(N_3)_3]\cdot CH_3OH\}_n$, and for compound **3** the X-ray formula is $\{[Cu_2(H_2L)(N_3)_3][ClO_4]\}_n$ and the analysis formula is $\{[Cu_2(H_2L)(N_3)_3][ClO_4]\cdot 0.8CH_3OH\}_n$. So, in compounds **1**−**3** the CHN analysis shows 0.7, 1.0, and 0.8 molecules of methanol, respectively, because the analysis was carried out on the samples that were just air-dried (because of their potential explosive nature).

$\{[Cu_2(H_2L)(N_3)_3]\cdot H_2O\cdot 0.7CH_3OH\}_n$ (1). 2,6-Diformyl-4-methylphenol (DFMP; 0.085 g, 0.50 mmol) dissolved in hot methanol (15 mL) was added to a solution of 2-aminoethanol (0.060 g, 1.0 mmol) in methanol (15 mL). The yellow solution of the Schiff-base ligand (H_3L) formed was refluxed for ca. 30 min. $Cu(CH_3CO_2)_2\cdot H_2O$ (0.20 g, 1.00 mmol) dissolved in hot methanol (50 mL) was added to the solution of the Schiff-base ligand, dropwise with stirring at ca. 60 °C. The brown solution formed initially changed to green in about 5 min. The resulting green solution was refluxed for ca. 10 min, and a solution of NaN_3 (0.065 g, 1.0 mmol) in a methanol/water mixture (8 + 2 mL) was added dropwise. The color of the reaction mixture changed to dark green, and the reaction mixture was refluxed further for ca. 10 min and filtered hot. To the filtrate was added a solution of CH_3CO_2Na (0.820 g, 10.0 mmol) in methanol (15 mL), and the mixture was left unperturbed for slow evaporation. After about 2 weeks, dark-green crystals suitable for X-ray studies were obtained and were kept in the mother liquor. The crystals of the bulk sample were separated from the mother liquor, washed with methanol (3 × 3 mL), and air-dried at ambient temperature. Yield: 0.14 g, 56%. Elem anal. (air-dried sample). Calcd for $[Cu_2(H_2L)(N_3)_3]\cdot H_2O\cdot 0.7CH_3OH$: C, 30.31; H, 4.05; N, 28.38. Found: C, 30.54; H, 4.02; N, 28.24.

$\{[Cu_2(H_2L)(N_3)_3]\cdot CH_3OH\}_n$ (2). Compound **2** was obtained in a manner similar to that of compound **1**. In this case, after the addition of the NaN_3 solution to the reaction mixture of DFMP, 2-aminoethanol, and $Cu(CH_3CO_2)_2$, the mixture was further refluxed for ca. 10 min and left at room temperature for slow evaporation. After a few days, a green powder separated from the dark-green solution, which was filtered off and discarded. The filtrate was kept at room temperature for slow evaporation, and after ca. 1 week, very nice crystals suitable for X-ray studies separated from the solution. The crystals used for X-ray studies were kept in the mother liquor. The remaining crystals were separated and washed with methanol (2 × 2 mL). The crystals crumble to form a parrot-green powder when taken out of the mother liquor. Yield: 0.15 g, 60%. Elem anal. Calcd for $[Cu_2(H_2L)(N_3)_3]\cdot CH_3OH$: C, 31.46; H, 3.96; N, 28.83. Found: C, 31.79; H, 3.79; N, 29.09.

$\{[Cu_2(HL)(N_3)](ClO_4)\cdot 0.8CH_3OH\}_n$ (3). Compound **3** was prepared by the same method as that used for **1**, by replacing $Cu(CH_3CO_2)_2\cdot H_2O$ with $Cu(ClO_4)_2\cdot 6H_2O$. In this case, after the addition of NaN_3 dissolved in a water/methanol (5 mL + 5 mL) mixture, the mixture was refluxed for ca. 30 min. Dark-green crystals suitable for X-ray analysis were obtained by slow (ca. 2 weeks) evaporation of the reaction mixture. Yield: 0.18 g, 70%. Elem anal. (bulk air-dried sample). Calcd for $[Cu_2(HL)(N_3)](ClO_4)\cdot 0.8CH_3OH$: C, 30.55; H, 3.57; N, 12.91. Found: C, 30.26; H, 3.10; N, 12.46. During the course of this investigation, this compound was very recently reported by another group,[50] and therefore the structure will be dealt with only in the Supporting Information.

$[Cu_2(HL)(N_3)_2(H_2O)]\cdot 0.5CH_3OH$ (4). Compound **4** was obtained by a method similar to that used for compound **1**. In this case, after the addition of NaN_3 dissolved in a water/methanol (6 mL + 4 mL) mixture, the reaction mixture of DFMP (1.00 mmol), 2-aminoethanol (2.00 mmol), $Cu(CH_3CO_2)_2$ (2.00 mmol), and NaN_3 (2.00 mmol) was further refluxed for ca. 1.5 h. A parrot-green solid separated from a dark-green solution, which was collected by filtration after cooling and washed with methanol (3 × 3 mL). It was air-dried at ambient temperature. Yield: 0.31 g, 63%. Despite several attempts, crystals suitable for X-ray diffraction were not obtained in this case. Elem anal. Calcd for $[Cu_2(HL)(N_3)_2(H_2O)]\cdot 0.5CH_3OH$: C, 32.86; H, 4.09; N, 22.71; Cu, 25.76. Found: C, 32.89; H, 3.76 ; N, 22.51; Cu, 26.12.

X-ray crystallography. A dark-green crystal of compound **1** was mounted onto a thin glass fiber and immediately placed under a liquid-N_2-cooled N_2 stream on a Bruker AXS platform single-crystal X-ray diffractometer upgraded with an APEX II CCD detector. The radiation used was graphite-monochromatized Mo Kα radiation (λ = 0.7107 Å). The lattice parameters

(50) Dhara, K.; Karan, S.; Ratha, J.; Roy, P.; Chandra, G.; Manassero, M.; Mallik, B.; Banerjee, P. *Chem.—Asian J.* **2007**, *2*, 1091–1100.
(51) Ullman, F.; Brittner, K. *Chem. Ber.* **1909**, *42*, 2539–2549.

Table 1. Summary of Crystallographic Data for Compounds **1**−**3**[a]

compound	**1**	**2**	**3**
empirical formula	$C_{13}H_{19}Cu_2N_{11}O_4$	$C_{13}H_{17}Cu_2N_{11}O_3$	$C_{13}H_{16}ClCu_2N_5O_7$
M	520.47	502.46	516.84
cryst syst	monoclinic	monoclinic	orthorhombic
space group	$P2_1/c$	$P2_1/c$	$Pbca$
a/Å	12.1834(10)	9.434(4)	8.7634(14)
b/Å	22.8445(18)	20.618(9)	18.041(3)
c/Å	6.9771(6)	10.040(4)	21.515(4)
β/deg	102.7070(10)	102.587(6)	
V/Å^3	1894.3(3)	1905.9(14)	3401.6(9)
ρ_{calcd}/(g cm^{-3})	1.825	1.751	2.018
T/K	130(2)	100(2)	100(2)
Z	4	4	8
μ/mm^{-1}	2.295	2.274	2.710
cryst size (mm)	0.34 × 0.25 × 0.19	0.30 × 0.24 × 0.18	0.19 × 0.11 × 0.09
reflns collected:			
total	15016	14702	18634
unique	3353	3369	3012
R_{int}	0.0319	0.04131	0.1166
final R1, wR2	0.0246, 0.0809	0.0338, 0.1087	0.0508, 0.1281

[a] R1 = $\sum[|F_o| - |F_c|]/\sum|F_o|$, wR2 = $[\sum[w(|F_o|^2 - |F_c|^2)^2]/\sum[w(|F_o|^2)^2]]^{1/2}$. R = $\sum||F_o| - |F_c||/\sum|F_o|$, R_w = $[\sum w(|F_o| - |F_c|)^2/\sum wF_o^2]^{1/2}$. NB: lattice MeOH has been excluded in the table.

were optimized from a least-squares calculation on carefully centered reflections. Lattice determination, data collection, data reduction, and structure refinement were carried out using the *APEX2* version 1.0-27 software package.[52,53] The data were corrected for absorption using the *SCALE* program within the *APEX2* software package.[52,53] Each structure was solved using direct methods. This procedure yielded Cu atoms, along with a number of C, N, and O atoms. Subsequent Fourier synthesis yielded the remaining atom positions. The H atoms are fixed in positions of ideal geometry (riding model) and refined within the *SHELXL* software package.[54] These idealized H atoms had their isotropic temperature factors fixed at 1.2 or 1.5 times the equivalent isotropic U of the C atoms to which they were bonded. A few H atoms could not be adequately predicted via the riding model within the *SHELXL* software.[54] These H atoms were located via difference Fourier mapping and subsequently refined. The final refinement of each compound included anisotropic thermal parameters on all non-H atoms. The crystal data for compounds **1**−**3** are given in Table 1. Selected interatomic distances and angles are listed in Tables 2, 3, and S1 in the Supporting Information.

Results and Discussion

Description of Structures. $\{[Cu_2(H_2L)(N_3)_3]\cdot H_2O\cdot 0.7CH_3OH\}_n$ (1). The single-crystal X-ray diffraction study shows that the structure of **1** consists of a 1D single chain resulting from the bridging of the dinuclear units $[Cu_2(H_2L)(N_3)]^{2+}$ through double EO azido anions. The molecular structure of centrosymmetric complex **1** is shown in Figure 2, together with relevant atomic labeling, and important bond distances and angles are listed in Table 2.

In compound **1**, H_3L acts as a tridentate (N_2O) monoanionic ligand (H_2L^-) binding through two imine N atoms and a deprotonated phenoxide O atom, thereby bridging two Cu^{II} ions into a dinuclear unit. The ethanol groups of the Schiff-base ligand's side arms remain protonated and uncoordinated. In each dinuclear unit, two

Table 2. Bond Distances [Å] and Angles [deg] for **1**

bond	length	bond	angle
Cu1−N1	1.959(2)	N1−Cu1−N9	95.06(9)
Cu1−N3	1.972(2)	N1−Cu1−N9	95.06(9)
Cu1−N9	1.984(2)	N3−Cu1−N9	96.00(9)
Cu1−O1	2.0067(16)	N1−Cu1−O1	92.73(8)
Cu1−N6	2.424(2)	N3−Cu1−O1	76.64(8)
Cu2−N6A	1.969(2)	N9−Cu1−O1	152.89(9)
Cu2−N2	1.974(2)	N1−Cu1−N3	168.83(8)
Cu2−N3	1.974(2)	N6A−Cu2−N2	94.36(9)
Cu2−O1	1.9897(17)	N6A−Cu2−N3	96.55(9)
Cu2−N9A	2.574(3)	N2−Cu2−O1	91.78(8)
Cu1−Cu2	3.112(3)	N3−Cu2−O1	76.98(8)
Cu1−Cu2A	3.969(3)	N2−Cu2−N3	168.74(8)
		N6A−Cu2−O1	161.85(9)
		Cu2−O1−Cu1	102.27(8)
		Cu1−N3−Cu2	104.09(10)
		Cu2A−N6−Cu2	110.25(10)

Cu^{II} ions are bridged through a phenoxide O atom and a μ-azido(N1,N1) bridge. A perspective view of the polymeric unit along the b axis is presented in Figure 3.

The stereochemistry at each Cu^{II} ion can best be described as a distorted square pyramidal with phenoxido O, imine N, and two azido N atoms in the equatorial plane and an azido N atom in the axial plane, with Cu1 being much more distorted than Cu2 (τ = 0.27 and 0.11, respectively).[55] The sums of the angles in the basal plane of Cu1 and Cu2 are 360.43(8)° and 359.67(8)°, respectively, indicating planar arrangements around these metal centers. The Cu−N and Cu−O bond distances in the basal plane lie in the ranges 1.959(2)−1.984(2) and 1.9897(17)−2.0067(16) Å, respectively. The dinuclear units are linked through two relatively longer Cu−N(azide) bonds that lie in the range 2.42(2)−2.57(4) Å to form 1D alternating single chains. In a dinuclear unit, the bridge angles at the phenoxide O atom (O1) and azide N atom (N3) are 102.27(8)° and 104.09(10)°, respectively. The sums of the angles around the phenoxide-bridging O atom (O1) and the azide-bridging N atom (N3) are 359.85(10)° and 357.74(15)°, respectively, indicating fairly planar arrangements at these

(52) Bruker, A. *SAINT 6.45A*; Bruker Analytical X-ray Systems: Göttingen, Germany, 2003; Vol. 6.
(53) Bruker, A. *APEX II*; Bruker Analytical X-ray Systems: Göttingen, Germany, 2005; Vol. II.
(54) Bruker, A. *SHELXTL V6.12*; Bruker Analytical X-ray Systems: Göttingen, Germany, 2002; Vol. 6.
(55) Addison, A. W.; Rao, T. N.; Reedijk, J.; van Rijn, J.; Verschoor, G. C. *J. Chem. Soc., Dalton Trans.* **1984**, 1349.

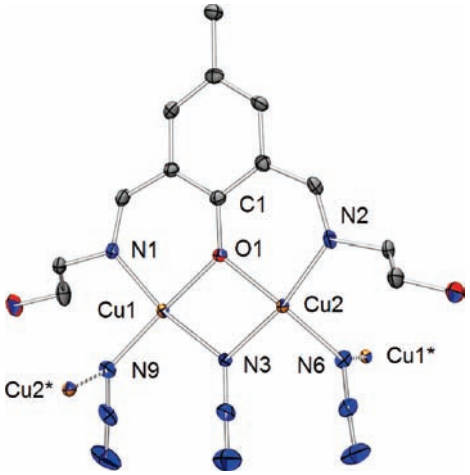

Figure 2. Molecular structure and numbering used for the dinuclear unit in the 1D single chain of **1**. Only equatorial ligands are shown for Cu.

Table 3. Bond Distances [Å] and Angles [deg] for **2**

bond	length	bond	angle
Cu1−N10	1.970(3)	N10−Cu1−N4	96.82(13)
Cu1−N4	1.982(3)	N4−Cu1−N1	92.08(12)
Cu1−N1	1.995(3)	N10−Cu1−O1	92.29(11)
Cu1−O1	2.008(2)	N1−Cu1−O1	76.74(11)
Cu1−N7A	2.434(3)	N10−Cu1−N1	168.84(12)
Cu1−N6	2.743	N4−Cu1−O1	168.74(12)
Cu2−N11	1.965(3)	N11−Cu2−N7	97.42(13)
Cu2−N7	1.988(2)	N11−Cu2−O1	92.51(11)
Cu2−O1	1.992(2)	N7−Cu2−N1	92.32(12)
Cu2−N1	1.993(3)	O1−Cu2−N1	77.15(11)
Cu2−O3A	2.399(2)	N7−Cu2−O1	167.01(11)
Cu2−N1	2.641(3)	N11−Cu2−N1	169.08(12)
Cu1−Cu2	3.125(3	Cu1−O1−Cu2	102.76(11)
Cu1−Cu2A	3.379(3)	Cu1−N1−Cu2	103.20(12)
		Cu2−N7−Cu1A	99.13(12)
		Cu1−N1−Cu2A	92.50(20)
		Cu2−N1−Cu2A	100.08(20)

atoms to allow effective magnetic exchange interaction between the Cu1 and Cu2 ions in the dinuclear unit.

The bridge angles at O1 and N3 would suggest an antiferromagnetic and a ferromagnetic spin coupling, respectively, between Cu centers within the dinuclear units.[41,56] The bridging angles at the μ-N_3(N1,N1) atoms N6 and N9 are 110.25(10)° and 120.53(10)°, respectively, suggesting that a strong antiferromagnetic spin-exchange interaction would be expected between Cu ions of the dinuclear units in such a 1D polymeric chain.[12] The sums of the angles at N6 and N9 are 347.25° and 349.20°, respectively, indicating some pyramidal distortion. The Cu1−Cu2 distance of 3.112 Å in each dinuclear unit is similar to the distance found in other dinuclear and tetranuclear copper, cobalt, and nickel complexes with similar ligands.[57−60] The

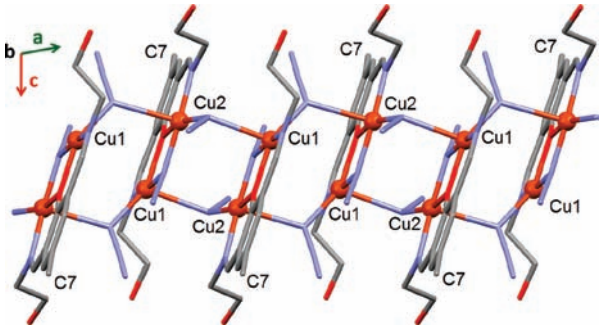

Figure 3. Perspective view of the crystal packing of **1** as seen along the *b* axis.

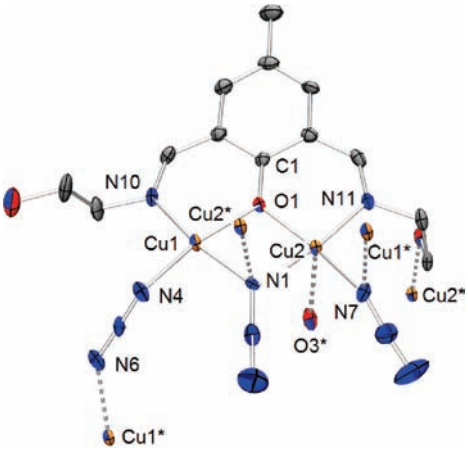

Figure 4. View of a dinuclear unit with relevant numbering added in a tetranuclear fragment in **2**.

Cu1−Cu2A distance between dinuclear units that are bridged through the μ-azido(N1,N1) bridge is 3.613 Å, which is significantly longer than the intermetallic separation within dinuclear units.

{[$Cu_2(H_2L)(N_3)_3$]·CH_3OH}$_n$ (2). Compound **2** features basic $[Cu_2(H_2L)(N_3)]^{2+}$ building blocks analogous to **1** with both metals bridged by one EO azido ligand and the phenoxide O atom of H_2L^-. These dinuclear units occur as centrosymmetric dimers because the azido ligand within the Cu_2 unit is also coordinated to one Cu^{II} center from the neighboring dinuclear entity, thereby exhibiting the μ_3-N_3(N1,N1,N1) coordination mode. The link between Cu_2 pairs is completed by two additional azide groups coordinating in a μ-N_3(N1,N1) fashion. The resulting dinuclear unit is shown in Figure 4; these units are arranged in tetranuclear clusters bridging to four other such units, thus forming a 2D network contained within the crystallographic *ac* plane, as shown in Figure 5.

This network is made up of a grid where the tetranuclear nodes are connected via double EE μ_3-N_3(N1,N1, N1) bridges along the *c* crystallographic direction and through two OH groups from the ethanol arms of the H_2L^- ligands along the *a* axis (see Figure 5). The sheets are packed in the direction of the *b* axis by means of van der Waals and hydrogen-bonding interactions (see below). There are thus three types of azido-bridging ligands present in compound **2**; EO μ_3-N_3(N1, N1,N1) (as a bridge within the Cu_2 units and pairing

(56) Thompson, L. K.; Tandon, S. S.; Manuel, M. E.; Park, M. K.; Handa, M. Magnetostructural correlations in dinuclear Cu(II) and Ni(II) complexes bridged by μ-1,1-azide and μ-phenoxide. In *Molecule-Based Magnetic Materials—Theory, Techniques, and Applications*; Turnbull, M. M., Sugimoto, T., Thompson, L. K., Eds.; American Chemical Society: Washington, DC, 1996; Vol. 644, pp 170−186.
(57) Mandal, D.; Ray, D. *Inorg. Chem. Commun.* **2007**, *10*, 1202–1205.
(58) Mukherjee, S.; Weyhermuller, T.; Bothe, E.; Chaudhuri, P. *Eur. J. Inorg. Chem.* **2003**, 1956–1965.
(59) Mukherjee, S.; Weyhermuller, T.; Bothe, E.; Wieghardt, K.; Chaudhuri, P. *Eur. J. Inorg. Chem.* **2003**, 863–875.
(60) Zhang, W. X.; Ma, C. Q.; Wang, X. N.; Yu, Z. G.; Lin, Q. J.; Jiang, D. H. *Chin. J. Chem.* **1995**, *13*, 497–503.

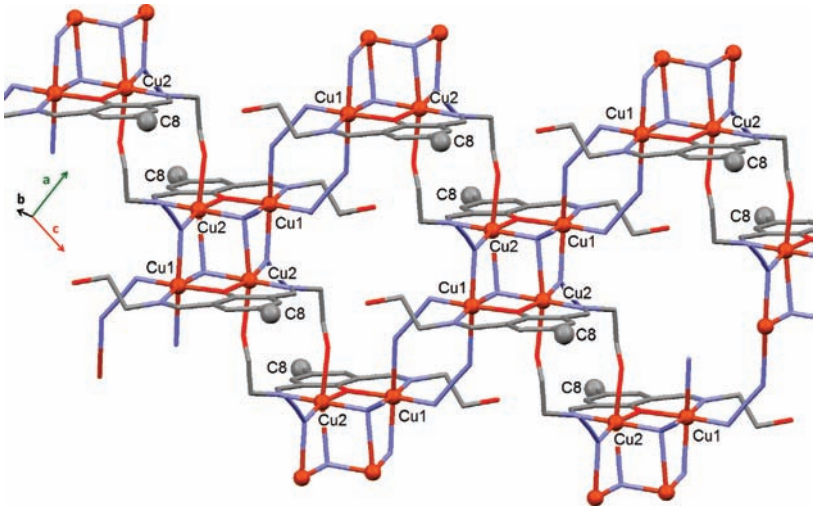

Figure 5. Perspective view of the crystal packing of **2** along the *b* axis, showing the tetranuclear units.

them), EO μ-N_3(N1,N1) (completing the link between Cu_2 fragments), and EE μ-N_3(N1,N1) (linking the resulting tetranuclear units into the polymeric network). In turn, the ligand H_2L^- chelates and bridges two Cu^{II} ions as in **1**, while one of its hydroxyethyl arms is engaged in coordination interactions with neighboring tetranuclear nodes, helping to establish the 2D lattice. The other arm remains uncoordinated and is involved in a hydrogen bond with the terminal N atom of a EO μ-N_3(N1,N1) group from a neighboring sheet.

The relevant bond distances and angles are listed in Table 3. The stereochemistry at each Cu^{II} ion can be described as a distorted octahedral. The coordination environment at the basal plane of Cu1 consists of a phenoxide O atom (O1), an imine N atom (N10), and two azido N atoms (N1 and N4), with azido N atoms (N6A and N7) at the axial positions. The coordination core of Cu2 in the equatorial plane consists of a phenoxide group (O1), an imine moiety (N11), and two azido N atoms (N1 and N7), whereas an azido N atom (N1A) and a hydroxyethyl O atom (O3a) from the next tetranuclear unit completes the axial coordination. The sums of the angles in the basal plane of Cu1 and Cu2 are 359.93(12)° and 359.40(11)°, respectively, indicating planar arrangements at these metal centers. The Cu−N and Cu−O bond distances in the basal plane of Cu1 and Cu2 lie in the ranges 1.965(3)−1.995 (3) and 1.992(2)−2.008(2) Å, respectively. The Cu1−N7A and Cu1−N6A axial distances are 2.434(3) and 2.743 Å, respectively. The axial distances for Cu2 are Cu2−O3A = 2.399(2) Å and Cu2−N1A = 2.641 Å. In a dinuclear unit of **2**, the bridge angles at the phenoxido O atom (O1) and the azido N atom (N1) are 102.76(11)° and 103.20(12)°, respectively. The sums of the angles at the O atom of the phenoxido bridge (O1) and the N atom of the azido bridge (N1) are 359.16(5)° and 349.10(5)°, respectively, indicating μ-planar and distorted μ-pyramidal binding modes. The bridge angles at the μ-N_3(N1,N1) atom (N7) and the μ_3-N_3(N1,N1,N1) atom (N1) bridging two dinuclear units are 99.13(12)° and 92.50°, respectively, suggesting magnetic spin-exchange interactions between Cu ions in tetranuclear units of a 1D polymeric chain. The sum of the angles at N7 is 359.83(3)°, indicating a planar arrangement around azide N (μ-planar) for effective spin-exchange interactions between Cu centers of the tetranuclear core. The Cu1−Cu2 distance of 3.125 Å in a dinuclear unit is similar to the distance found in **1** and other dinuclear copper complexes with similar ligands.[57−60] The Cu1−Cu2A distance of 3.379 Å in the tetranuclear core is significantly shorter than that observed in **1** but much longer compared to the Cu−Cu distance within dinuclear units.

$\{[Cu_2(HL)(N_3)]ClO_4\cdot 0.8(CH_3OH)\}_n$. Compound **3** crystallizes in the orthorhombic space group *Pbca*. It consists of a 2D coordination polymer comprised of repeating dinuclear units cross-linked to form sheets. During the course of the writing, the structure was published,[50] albeit it at a different temperature and with a lower resolution. The details of the structure description are given in the Supporting Information, together with a drawing and a packing diagram.

IR and UV−Vis Spectroscopy. In the IR spectrum of **1**, which has EO intradimer and interdimer (μ-1,1) bridging azide groups, three bands are observed at 2086, 2061, and 2041 cm^{-1}, typical for such bridging moieties.[42] The IR spectrum of **2**, which has three different types (μ-1,1-N_3, μ_3-1,1,1-N_3, and μ-1,3-N_3) of bridging azides, shows two strong bands at 2091 and 2015 cm^{-1}. In the IR spectrum of **3**, which has only one type of EO bridging azide, only one band at 2092 cm^{-1} is observed. The small splittings of the ClO_4^- ion band (1111, 1094, 1056, and 1025 cm^{-1}) are indicative of a weak interaction of perchlorate with Cu1 at one axial position and hence a distortion from regular symmetry. The two bands in the region 1629−1655 cm^{-1} are due to the $\nu_{C=N}$ stretch of coordinated imine groups. In the IR spectrum of **4**, which is proposed to have two azide ions per dinuclear unit, two strong bands are present (2092 and 2017 cm^{-1}) at nearly the same positions as those observed for **2**, indicating that **4** might have a similar structure.

The UV−vis spectra of all four compounds, recorded in the solid state, are characterized by a strong band at 400 nm, which is ascribed to a copper azide charge-transfer band. On this band, low-energy shoulders are visible at 500, 440, 440, and 450 nm for compounds **1**−**4**, respectively, tentatively also assigned to Cu−L charge transfer.

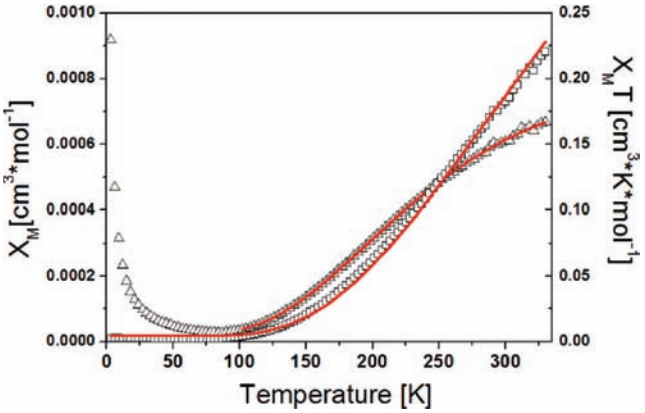

Figure 6. Plots of $\chi_M T$ (squares) and χ_M (triangles) vs T per mole of Cu_2 unit for **1**. The solid lines are the fits to the experimental data for T higher than 100 K.

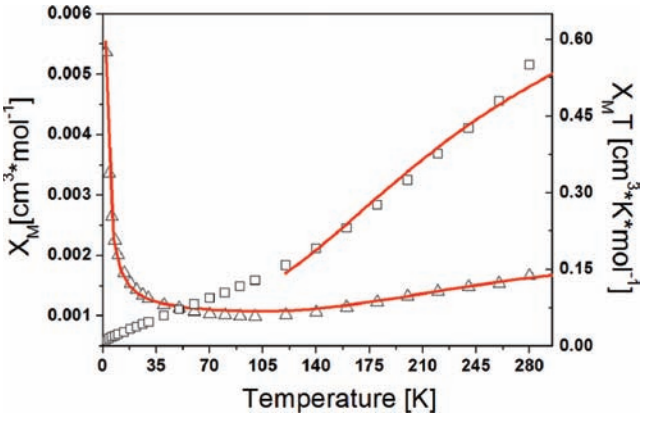

Figure 7. Plots of $\chi_M T$ (squares) and χ_M (triangles) vs T per mole of Cu_2 unit for **2**. The solid lines are the fits to the experimental data for T higher than 120 K.

The d−d transitions characteristic of Cu^{II} are observed as broad bands at 700, 720, 620, and 750 nm, respectively, typical for octahedrally based geometry.[61]

Magnetic Properties. The fact that the compounds all have quite short Cu−Cu distances with bridging ligands is likely to result in magnetic interactions. No useful features could be derived from electron paramagnetic resonance (broad lines only even down to very low T), and only magnetic susceptibility has been used for a detailed study. The $\chi_M T$ and χ_M vs T plots for compounds **1**−**3** under a constant magnetic field of 0.1 T are shown in Figures 6−8, respectively. For the three compounds, the curves are very similar; the χ_M value per mole of Cu_2 dimer at 300 K is $6.67 \times 10^{-4}/1.78 \times 10^{-3}/1.34 \times 10^{-3}$ $cm^3\ mol^{-1}$ (in the **1**/**2**/**3** format) and decreases with cooling to a minimum at 55/65/75 K, increasing again at lower

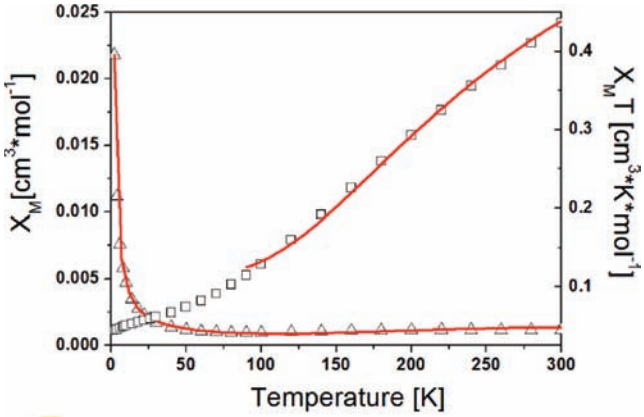

Figure 8. Plots of $\chi_M T$ (squares) and χ_M (triangles) vs T per mole of Cu_2 unit for **3**. The solid lines are the fits to the experimental data for T higher than 90 K.

temperatures because of the presence of paramagnetic impurities. The $\chi_M T$ products at 300 K are 0.17/0.62/0.64 $cm^3\ K^{-1}\ mol^{-1}$. These values are lower than expected for two uncoupled Cu^{II} ions (0.75 $cm^3\ K^{-1}\ mol^{-1}$ for $g = 2$). These values and the shape of the curves indicate that the magnetic coupling is dominated by strong antiferromagnetic interactions. Data are summarized in Table 4, together with literature data to be discussed below.

Inspection of the structures suggests that the strong antiferromagnetic coupling is mediated through the PhO^- and N_3^- bridges within the Cu_2 basic units present in the three complexes, which involve all equatorial positions of the metals. Any other possible magnetic pathways, except one, will pass through at least one axial Cu−L bond, which represents a weak link in terms of the magnetic exchange. The only interdimer pathway occurring via two equatorial bonds is mediated by a single alkoxide bridge (see above, complex **3**), with the planes of the magnetic orbitals ($d_{x^2-y^2}$) of the Cu^{II} ions being quasi-perpendicular, which should weaken significantly the interaction. Thus, we have reduced modeling of the magnetization data of these compounds to the problem of estimating the magnitude of the strong antiferromagnetic coupling within the discrete dinuclear entities, with any other possible interaction being masked by this single pathway. Consequently, the magnetic susceptibility data of the three complexes were fitted to the Bleaney−Bowers equation[67] for two interacting Cu^{II} ions using the Hamiltonian $H = -JS_1 \cdot S_2$. The contributions of a paramagnetic impurity, ρ, and of temperature-independent paramagnetism (TIP) have been included in the model.[1] The fittings were performed by fixing g within the 2−2.3 interval. The effect of paramagnetic impurities appears often magnified at low temperatures in strongly antiferromagnetic compounds. In order to decrease these perturbing effects, only the data above 100, 120, and 90 K were included in the fits. The resulting best-fit parameters were $J = -512(1)/-330(20)/-347(3)/\ cm^{-1}$, $g = 2/2.3/2$, $\rho = 2/5/14\%$, TIP = $(120/60/60) \times 10^{-6}\ cm^3\ mol^{-1}$, and $R = 2 \times 10^{-6}/0.96/3 \times 10^{-5}$ (again using the **1**/**2**/**3** format). The solid lines in Figures 6−8 correspond to

(61) Hathaway, B. J. *Comprehensive Coordination Chemistry*; Pergamon Press: Oxford, U.K., 1987; Vol. 5.
(62) Lorosch, J.; Paulus, H.; Haase, W. *Inorg. Chim. Bioinorg.* **1985**, *106*, 101–108.
(63) Mallah, T.; Boillot, M. L.; Kahn, O.; Gouteron, J.; Jeannin, S.; Jeannin, Y. *Inorg. Chem.* **1986**, *25*, 3058–3065.
(64) Mallah, T.; Kahn, O.; Gouteron, J.; Jeannin, S.; Jeannin, Y.; Oconnor, C. J. *Inorg. Chem.* **1987**, *26*, 1375–1380.
(65) Chattopadhyay, T.; Banu, K. S.; Banerjee, A.; Ribas, J.; Majee, A.; Nethaji, M.; Das, D. *J. Mol. Struct.* **2007**, *833*, 13–22.
(66) Kahn, O.; Mallah, T.; Gouteron, J.; Jeannin, S.; Jeannin, Y. *J. Chem. Soc., Dalton Trans.* **1989**, 1117–1126.
(67) Bleaney, B.; Bowers, K. D. *Proc. R. Soc. London, Ser. A* **1952**, *214*, 451–61.

Table 4. Magnetochemical Parameters for the μ-Phenolatodicopper Complexes with μ-Azido as an Exogenenous Bridge[a]

compound	formula	Cu···Cu [Å]	Cu−OPh−Cu[deg]	α [deg]	$-J$ [cm^{-1}]	geometry	ref
1	$\{[Cu_2(H_2L)(N_3)_3]\cdot H_2O\cdot 0.7CH_3OH\}_n$	3.112	102.3	6.04	542	SP/SP	this work
2	$\{[Cu_2(H_2L)(N_3)_3]\cdot CH_3OH\}_n$	3.125	102.7	9.8	330	OC/OC	this work
3	$\{[Cu_2(HL)(N_3)]ClO_4\cdot 0.8(CH_3OH)\}_n$	3.042	101.1	9.7	347	SPL/SP	this work
4	$\{[Cu_2L^2(N_3)](ClO_4)_2\cdot(CH_3OH)\}_n$	3.12	102.9	5.3	534	SP/SP	62
5	$[Cu_2(Fdmen)(N_3)(ClO_4)_2]\cdot nH_2O$	2.972	98.7	20.04	87	OC/SP	63
6	$[Cu_2(Fmap)(N_3)](ClO_4)_2\cdot nH_2O$	2.993	100.5	7.01	161	OC/SP	64
7	$[Cu_2(L^3)(\mu\text{-}N_3)(N_3)_2]\cdot nH_2O$	3.032	101.3	12.3	188	OC/SP	65
8	$[Cu_2(L^4)(N_3)_2]\cdot nH_2O$	3.035	99.27	15.9	278	OC/OC	66

[a] SP: square pyramidal. OC: octahedral. SPl: square planar. L: this publication. L^2: Schiff base of 2-hydroxy-5-methylisophthalaldehyde and dimethylamino-1-propylamine. Fdmen: Schiff base of 2,6-diformyl-4-methylphenol with 1,1-dimethylethylenediamine. Fmap: 2,6-bis(*N*-(2-pyridylmethyl)formimidoyl)-4-methylphenolate. L^3: Schiff base of 4-methyl-2,6-diformylphenol and 1,2-diaminoethane. L^4: 4-methyl-2,6-bis[*N*-(2-methylthioethyl)formimidoyl]phenolate.

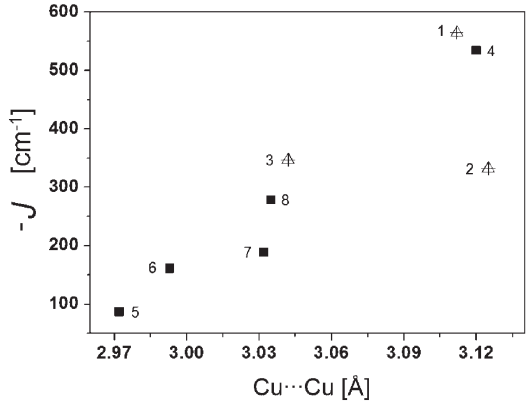

Figure 9. Plot of the antiferromagnetic interaction ($-J$) vs the Cu···Cu distance (d) in dinuclear μ-phenolato/μ-azido complexes.

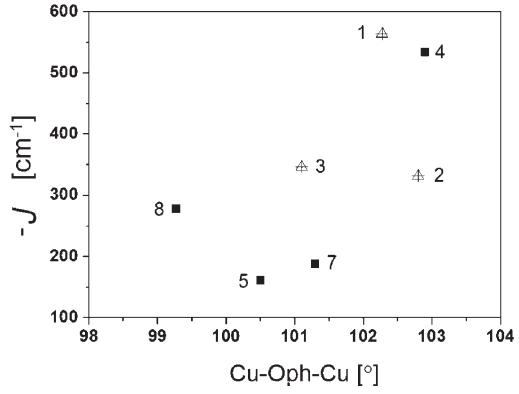

Figure 10. Plot of the antiferromagnetic interaction ($-J$) vs the Cu−OPh−Cu angle in dinuclear μ-phenolato/μ-azido complexes.

the theoretical curves obtained using the above parameters.

For compounds **2** and **3**, fits also were tried using a tetranuclear model, using an extra parameter J^2. In both, no better fits were obtained, and the chosen values for J^2 were found to be insensitive; e.g., for compound **3**, values from 0 to -500 cm^{-1} had little effect on the outcome; this can be understood from the fact that the magnetic orbitals are quite parallel, as seen from the packing diagrams.

Magnetostructural Correlations. For the three complexes, the strong antiferromagnetic interaction appears to occur within the $[Cu_2(OPh)(N_3)]$ core, where the short Cu−L bonds are found. The four bonds ensuring the bridging all take equatorial positions of Cu^{II} and are contained within the plane of the magnetic orbitals of both metals ($d_{x^2-y^2}$), which are approximately parallel. This arrangement is ideal for a very efficient magnetic coupling between the metals within the Cu_2 units, via the overlap of the copper magnetic d orbitals with the orbitals of the bridging atoms (O and N, respectively) hosting electron lone pairs. While EO azide ligands are known to mediate moderate ferromagnetic interactions,[3] the exchange is dominated by the phenoxide bridge, which has been shown to lead to very strong antiferromagnetic coupling.[68] In fact, the interaction mediated by the latter bridge has been studied from the theoretical and experimental points of view, and in both cases, well-defined correlations of the strength of the coupling with various parameters (especially the Cu−O−Cu angle θ) have been found.[68−70] We have gathered all compounds, and their magnetic data, from the literature that contain the $[Cu_2(OPh)(N_3)]$ core, together with the new compounds reported here, and have examined the relationship between the coupling constant J with a Cu···Cu distance d and θ. The results are presented in Figures 9 and 10 and summarized in Table 4.

Figure 9 clearly shows that for this category of compounds a reasonable correlation is seen between J and d. A possible origin for this correlation is that lengthening of d implies a concomitant opening of θ, for which previous studies indicate that this results in an increase of the antiferromagnetic character of the exchange.[68−70] This is indeed observed in a J vs θ plot for the compounds that we have investigated, although the correlation is much less defined (Figure 10). This poor correlation probably underscores the fact that there are always several other parameters in the system that have an influence on the magnetic exchange, such as the Cu−O distance, the exact coordination geometry of the metals, or the nature of the ancillary ligands. Therefore, it was decided to investigate the possible dependence of the constant J with the angle α formed between the ideal plane containing the bridging phenoxide group and the ideal plane of the four atoms of

(68) Thompson, L. K.; Mandal, S. K.; Tandon, S. S.; Bridson, J. N.; Park, M. K. *Inorg. Chem.* **1996**, *35*, 3117–3125.

(69) Ruiz, E.; Alemany, P.; Alvarez, S.; Cano, J. *Inorg. Chem.* **1997**, *36*, 3683–3688.

(70) Ruiz, E.; Alemany, P.; Alvarez, S.; Cano, J. *J. Am. Chem. Soc.* **1997**, *119*, 1297–1303.

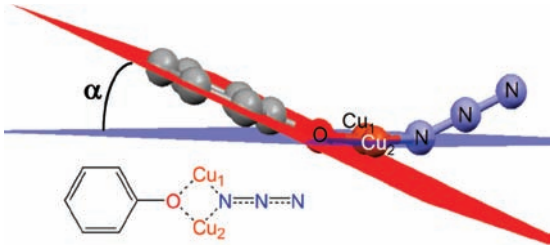

Figure 11. Definition of the angle α for the dinuclear μ-phenolato/μ-azido complexes.

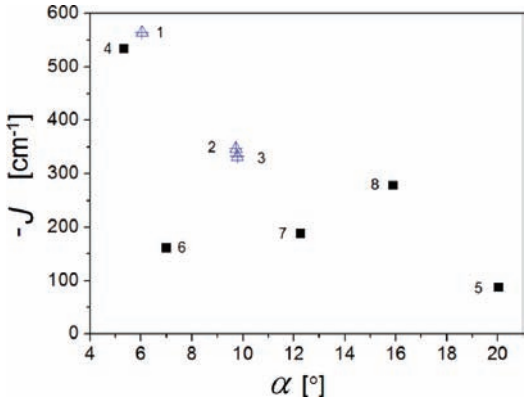

Figure 12. Plot of the antiferromagnetic interaction ($-J$) vs the angle α in dinuclear μ-phenolato/μ-azido complexes.

the [Cu(μ-O)(μ-N)Cu] core (Figure 11). The analogous angle for hydroxide-bridged Cu_2 complexes was predicted theoretically to influence the coupling because it affects the energy gap between the two singly occupied molecular orbitals involved in the singlet−triplet separation.[70] The results from the analysis of the experimental data are presented in Figure 12 and Table 4. Surprisingly, the reported compounds, together with compounds **1**−**3**, exhibit a rather distinct (inverse) trend between these two parameters, with the only remarkable deviation for compound **6**. As expected from density functional theory calculations, increasing the angle α would cause a decrease in the strength of the antiferromagnetic coupling. The deviation of complex **6** may be well explained by the fact that it is the system exhibiting a much larger *hinge* angle within the [Cu(μ-O)(μ-N)Cu] core (Cu−N−O−Cu torsion angle) that attenuates the intensity of the antiferromagnetic coupling.[70] To the best of our knowledge, the present study is the first clear correlation identified experimentally between J and the angle α within Cu_2 dinuclear magnetic units.

Conclusions

The capacity of the Schiff-base ligand 2,6-bis[[(2-hydroxyethyl)imino]methyl]-4-methylphenol (H_3L) to promote the formation of Cu_2 units has been demonstrated. Small variations in the reaction parameters of the system $H_3L/Cu^{II}/N_3^-$ allow for the preparation of different complexes exhibiting the [$Cu_2L(N_3)$] unit (L representing here H_3L at various degrees of deprotonation), organized in the crystal lattice as 1D or 2D polymers. The Cu_2 moieties exhibit both a phenoxide and an EO N_3^- bridge, while the polymers result from the presence of additional Cu−Cu bridging interactions via N_3^- groups or the alcohol arms of H_3L. The magnetic coupling within these frameworks is dominated by the strong antiferromagnetic interaction mediated by the phenoxide bridge within the Cu_2 moieties. The coupling constants, J, of these interactions have been estimated using the Bleaney−Bowers model. These, together with reported values from equivalent systems involving the same types of bridges, have been examined in relation to several structural parameters. From this analysis, a new magnetostructural correlation has emerged relating J with the angle α between the ideal plane of the phenoxide bridge and the ideal plane of the atoms in the Cu_2 core.

Acknowledgment. Kent State University at the Salem and East Liverpool Campuses (SST) and NSERC (LKT) are thanked for financial support. S.S.T. thanks Professor Roger Gregory, Chemistry Department, Kent State University at the Kent Campus for laboratory facilities and Dr. Mohinda Gangoda for assistance with spectroscopic and analytical studies. The work described in the present paper has been supported by the Leiden University Study group WFMO (Werkgroep Fundamenteeel-Materialen Onderzoek). Financial support and coordination by the FP6 Network of Excellence "Magmanet"(contract number 515767) are kindly acknowledged. The Ministry of Science and Education (Spain) is thanked for financial support.

Supporting Information Available: X-ray crystallographic files in CIF format for the structures of **1**−**3** and structure determination and details of the structure of compound **3**. This material is available free of charge via the Internet at http://pubs.acs.org. Crystallographic data (excluding structure factors) for the structures have also been deposited with the Cambridge Crystallographic Data Centre as supplementary publication nos. CCDC 703800−703802 for **1**−**3**, respectively. Copies of the data can be obtained, free of charge, via http://pubs.acs.org or upon application to CCDC, 12 Union Road, Cambridge CB2 1EZ, U.K. (fax +44-(0)1223−336033 or e-mail deposit@ccdc.cam.ac.uk).